

# COMPARISON OF THE CrN, TiN AND (Ti, Cr)N PVD COATINGS DEPOSITED BY CATHODIC ARC EVAPORATION

M. Akbarzadeh, A. Shafyei and H. R. Salimijazi

\* m.akbarzadeh110@yahoo.com

Received: June 2014

Accepted: August 2014

Department of Materials Engineering, Isfahan University of Technology, Isfahan, Iran.

**Abstract:** In the present study, CrN, TiN and (Ti, Cr)N coatings were deposited on D6 tool steel substrates. Physical and mechanical properties of coatings such as microstructure, thickness, phase composition, and hardness were evaluated. Phase compositions were studied by X-ray diffraction method. Mechanical properties were determined by nano-indentation technique. The friction and wear behaviour of the coatings were investigated using ball-on-disc tests under normal loads of 5, 7 and 9 N at sliding distance of 500 m, at room temperature. Scanning electron microscope equipped with energy dispersive spectroscopy, optical microscope, and 2D/3D profilometry were utilized to investigate the microstructures and wear mechanisms. Wear test results clarified that the wear resistance of (Ti, Cr)N and TiN coatings was better than that of CrN coating. The wear resistance of the (Ti, Cr)N coatings was related to the Ti content in the coatings and reduced by decreasing the Ti content. The dominant wear mechanisms were characterized to be abrasive and tribochemical wear.

**Keywords:** physical vapour deposition, thin films, wear resistance, Ti-Cr-N coating, characterization.

## 1. INTRODUCTION

In the past decade, transition coatings nitrides such as TiN and CrN, due to their low friction coefficient and high wear resistance, are used for protection of tool surfaces [1-5]. But today, the mechanical properties of these coatings cannot satisfy for modern cutting requirements. It is found that this problem may be solved by using metal/ceramic multilayered coatings that possess a high hardness as well as a high toughness when compared to the homogeneous coatings. Ternary nitrides have been investigated in order to answer the increasing need for superior conditions. Researches have been carried out into the development of new ternary nitrides comprised of transition elements. Multi-component Cr-X-N coatings, where X is the alloying elements such as, Pd [6], W [7], B [8], Si [1], Ta [9], Co [10], Mo [11], Al [12-14], and etc. have been explored in order to improve the properties of CrN coatings. Recently, it is reported that new ternary Cr-Ti-N coatings have high-temperature strength and corrosion resistance compared to CrN and TiN coatings. It has been reported that the corrosion resistance of Ti<sub>1-x</sub>Cr<sub>x</sub>N coatings at temperatures above 950°C increases with X and for X $\geq$ 0.3 it is equal to that for pure CrN [15-17].

Despite there have been many papers in the literature, studied about CrN, TiN and (Ti, Cr)N coatings properties, to our knowledge there have been a few studies that have tried to investigate characterization of (Ti, Cr)N and so far has not been studied seriously about its tribological properties. In the current study, CrN, TiN and (Ti, Cr)N coatings were deposited on D6 tool steel substrates. Physical and mechanical properties of coatings as well as wear and tribological behaviours were evaluated, comprehensively.

## 2. EXPERIMENTAL

The substrate AISI D6 tool steel rods with 50 mm diameter were cut in 5 mm thickness disks. The samples were annealed at 980°C followed by quenching in water and tempered at 180°C. The hardness of the sample was obtained 55 HRC. The substrates were strictly cleaned then ground and polished to the roughness (Ra) 0.01  $\mu$ m. Before deposition, in order to remove some adhering impurities on the substrates, the samples were heated and ion cleaned by metal ion bombardment under the following conditions:

time, 2 min, voltage, 600 V, temperature after treatment, 300 °C.

**Table 1.** CAE coating process parameters

parameters	value
Chamber volume (m <sup>3</sup> )	1
Working pressure (mbar)	10 <sup>-3</sup>
Cr evaporator current (A)	80, 300
Ti evaporator current (A)	300, 80
Distance between substrate and target (cm)	30
Deposition time (min)	60
Substrate temperature (°C)	150
Sample holder rotation speed (rpm)	20

Coatings were deposited by cathodic arc evaporation (CAE). Fig. 1 shows a schematic diagram of the deposition apparatus. (Ti, Cr) N coatings were deposited with two evaporation sources. Initially, chamber was evacuated to a pressure of 10<sup>-6</sup> mbar with a diffusion pump before introducing a reactive gas Cr (99.8% in purity) and Ti (99.6% in purity) target cathodes into a reactive nitrogen atmosphere at a nitrogen pressure of 2 Pa at bias voltage of -1000 V. CAE process parameters used in this investigation are tabulated in Table 1.

X-ray diffraction (XRD) technique was carried

out by using Philips PW-3710 diffractometer utilizing Cu K $\alpha$  radiation in the 2 $\theta$  range from 10 to 100 ° to evaluate the crystal structure, phase contents, and crystallographic orientations of coatings.

The mechanical properties such as the elastic modulus, E, and hardness, H, were measured by nanoindentation tester (TTX-NHT). This instrument records the load and displacement continuously. The mechanical properties of thin film coatings and substrates can be derived from measuring the load–displacement curve through by using the method of Oliver and Pharr [18]. The maximum indentation depth and load were 320 nm and 3000  $\mu$ N where maximum loading and unloading rate of 60.00 mN/min was applied. Six indentations on each coating were applied and the average values were presented.

The wear tests were performed using a ball-on-disk machine. This equipment is also controlled by its PC software, which allows seeing the evolution of the friction coefficient. The WC–6% Co ball (10 mm diameter) was loaded against the rotating sample with a normal load of 5, 7 and 9 N, while the sliding speed was 0.081 m/s. The sliding distance was 500 m. The applied loads were chosen according to the similar articles [19–22]. The frictional forces were continuously recorded during the test. The mass loss of the disk specimens was measured at a 100 m interval in sliding distance, with an analytical balance with 0.1 mg precision. After the wear tests, the wear tracks were examined using an optical 2D profilometry (Reflection Optical Microscope

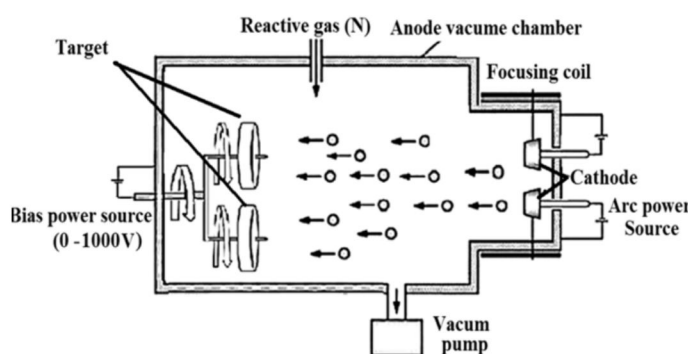


**Fig. 1.** A schematic illustration of a cathodic arc system.



Nikon) to measure the wear volume ( $\text{mm}^3$ ).

The worn surface and debris were evaluated using a Philips XL30 SEM with an EDS attachment. Before their microscopic studies, the samples were cleaned with a dry brush to eliminate a great amount of the material deposited on the wear track (debris) in order to obtain information only about the damage suffered by the coating.

### 3. RESULT AND DISCUSSION

The summary of deposition parameters, chemical composition and thickness of coatings is presented in Table 2. (Ti, Cr)N coatings have maximum thickness, since two target sources at equal coating times were used. After coating processes, the surface roughness of the samples was increased, which could be attributed to the CAV technique character and occurrence of the characteristic macro-droplets [23].

The XRD patterns of the TiN, CrN and

(Ti,Cr)N coatings are shown in Fig. 2. Coatings were highly textured with a preferential orientation in the (220) direction. Since thickness of coatings were less than  $5 \mu\text{m}$ , some peaks from the substrate can be detected as well [15].

CrN samples represent two stable modifications of chromium nitride: hexagonal  $\text{Cr}_2\text{N}$  and Cubic CrN. Whereas, TiN is stable over a broad range, CrN has a very narrow composition range and needs to use a very high partial pressure of nitrogen during deposition [24, 25]. Therefore, hexagonal  $\text{Cr}_2\text{N}$  could be easily observed under stoichiometric nitrogen conditions,  $\text{Cr}_2\text{N}$  diffraction peaks could be detected in the CrN and (Ti, Cr)N coatings. According to the X-ray diffraction pattern, it seems that the (Ti, Cr)N coating has only one solid solution cubic phase. The results of nano indentation test for coatings are shown in Table 3. Maximum hardness of approximately 29 GPa was obtained for TiN coating. The CrN coatings exhibited lower hardness and Young's modulus

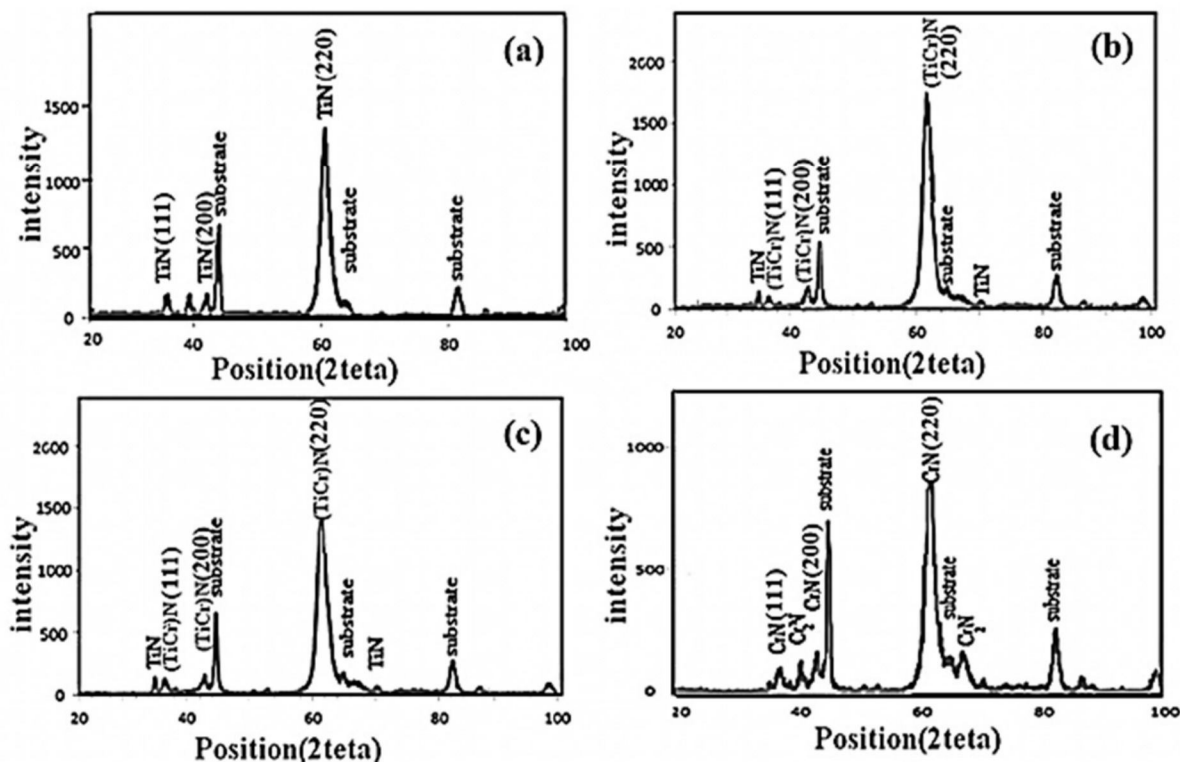


Fig. 2. X-ray diffraction patterns of the coatings.

**Table 2.** Deposition conditions and coating compositions.

Sample	Cr evaporator current(A)	Ti evaporator current (A)	Thickness ( $\mu\text{m}$ )	Substrate temperature ( $^{\circ}\text{C}$ )	Cr Content (Cr/(Cr + Ti))	Ti Content (Ti/(Cr + Ti))
a-1	0	300	2.1 $\pm$ 0.1	400	0	1
a-2	0	300	1.5 $\pm$ 0.1	100	0	1
b-1	80	300	2.8 $\pm$ 0.4	400	0.32	0.68
b-2	80	300	3.1 $\pm$ 0.1	100	0.35	0.65
c-1	300	80	3.5 $\pm$ 0.2	400	0.73	0.27
c-2	300	80	4.5 $\pm$ 0.2	100	0.70	0.30
d-1	300	0	2.8 $\pm$ 0.1	400	1	0
d-2	300	0	2.1 $\pm$ 0.1	100	1	0

**Table 3.** Result of nanoinditor test

Coating	<i>a</i>	<i>b</i>	<i>c</i>	<i>d</i>
Hardness (GPa)	28.5	26.0	22.3	17.1
Young's modulus (GPa)	360	415.9	373	273
Stiffness (N/m)	0.37	0.41	0.38	0.34

**Table 4.** Average of the worn volume, depth and width of the track.

sample	Depth of the wear track ( $\mu\text{m}$ )	Width of the wear track (mm)	Worn volume ( $\text{mm}^3$ )
a	0.78	1.09	0.080
b	1.05	1.10	0.109
c	1.00	1.27	0.120
d	2.22	0.89	0.186

values than other coatings. Considering the lower stiffness of TiN and CrN with respect to (Ti, Cr)N, this could be corresponded to a significantly lower compressive residual stresses during the growing process.

Fig. 3 shows optical 2D profilometry of the wear tracks on TiN coatings after 500m underat load of 7N. By using the optical profilometer, the average values from the worn volume, depth and width of the wear track of each coating were calculated and are shown in Table 4. Despite the (Ti, Cr)N sample has minimum nominal track width, it has the highest width and its worn volume is higher than other coatings which revealed that more material loss in the (Ti, Cr)N coating. The surface coating is rougher than wear track and wear track consisted of sharp edges in all coatings. "Having sharp edges in the wear track is the phenomenon of the coatings peeling off from the substrate because of the coating break" [26].

Fig. 4 shows evolution of the friction coefficient as a function of the sliding distance at load of 7N for coatings and substrate samples. All the friction

curves exhibited a similar pattern. The friction coefficient started at low values ( $\sim$ 0.2) and increased to reach to the highest values and then decreased until approached a steady-state with smaller friction coefficient values. The changes in the friction coefficient could be due to the removal of the surface film. For comparison purpose, experiments were also carried out to measure the friction coefficient of uncoated sample. The average friction coefficient of the substrate was 0.9 which was higher than other samples, so the applied coatings reduced the friction coefficient. At normal load of 7N after 200m, the friction coefficient variations with sliding distance was similar for the (Ti, Cr)N coatings.

First stage of wear test (running-in region) was not notable in CrN and TiN coatings, and the friction coefficient increased sharply iniially. Whilst in the (Ti, Cr)N coating, its amounts was low ( $\sim$ 0.2) and constant to approximately 50 and 100m.

The friction coefficient of (Ti, Cr)N coatings was the lowest, whilst the friction coefficient of CrN coating was the highest amongst three



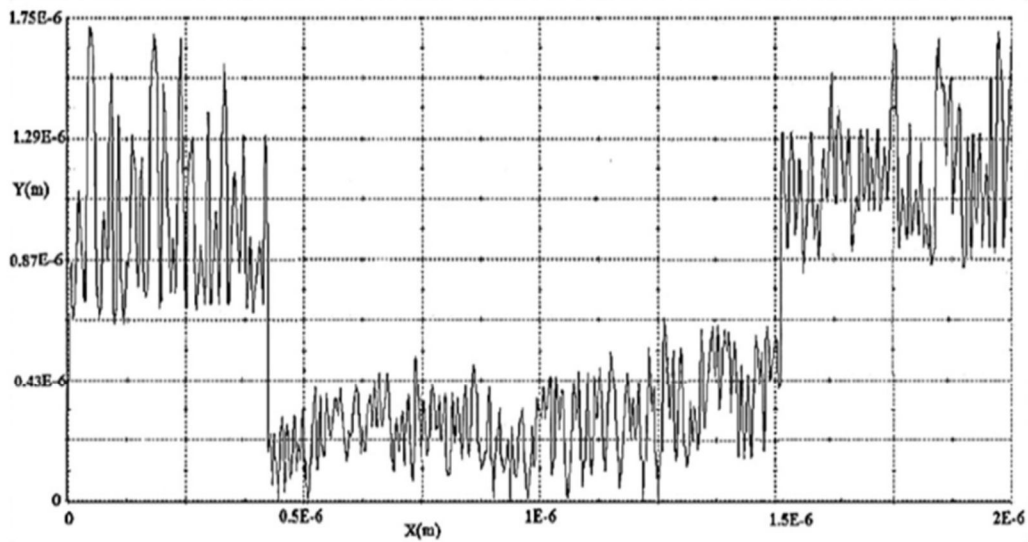


Fig. 3. Optical 2D morphologies of the wear track for (Ti, Cr)N coating.

coatings tested at the applied load of 7N. The domain fluctuations in the friction coefficient of (Ti, Cr)N at the load of 7N was less than two TiN and CrN. Perhaps, because of the low amount of the particles produced during the wear that lead to conflict and locking of ball and abrasive wear. At this study, normal load truly affects the friction coefficient and wear volume. The variations of the steady state friction coefficient as a function of the applied normal load is presented in Fig. 5. The results indicated that, the coefficient of friction was reduced because of coatings, however, the surface roughness was

increased (Table 2). The (Ti, Cr)N coating exhibited the highest average steady state friction coefficient. The dependence of the friction coefficient on the applied load in the uncoated steel was not so significant and nearly constant. The friction coefficient of TiN coatings decreased with increasing in the applied normal load between 7 and 9, therefore, the (Ti, Cr)N and CrN coatings behavior was in contrast with TiN coating. This observation cannot be explained by the friction mechanism in the micro scale. The coefficients of friction are made up of contributions from the deformation of the surface

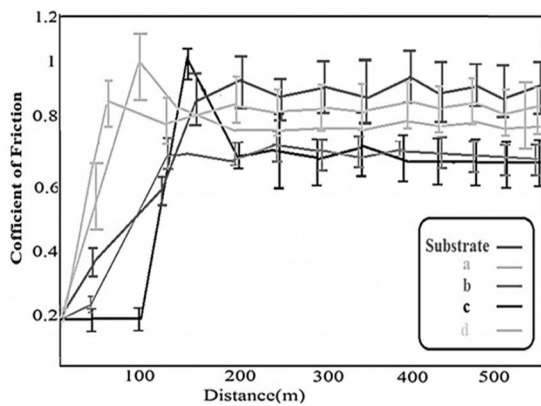


Fig. 4. Variation of the friction coefficient under loads of 7N for the coatings and substrate.

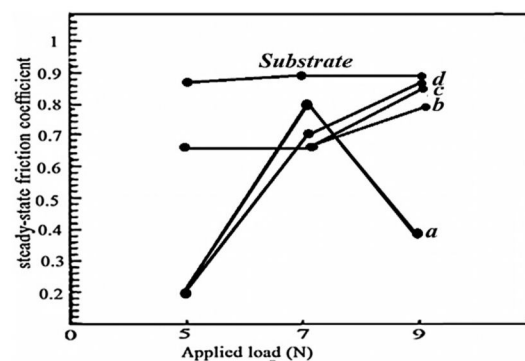


Fig. 5. The average steady friction coefficient as a function of the applied load.

asperities, ploughing, and adhesion. At the applied load of 9N, ploughing mechanism was dominated and tribochemical layer cannot be created whilst this layer was formed at the applied load of 7N and mechanism of asperity deformation and adhesion was activated. Therefore the steady state friction coefficient was increased [23, 24].

For specimens coated with CrN film, their wear volumes increased nearly linearly with an increase in the sliding distance. For specimens coated with (Ti, Cr)N and TiN film, their wear volumes increased linearly logarithmically and constant after 300m.

The (Ti, Cr)N coatings showed lower the coefficient of friction and their wear volume were higher than those of TiN coatings due to their differences in their wear mechanisms (see Fig 6). The wear resistance of TiN coatings was much higher than that of other two coatings.

In order to determine dominant wear mechanisms at the normal loads of 7N, the wear tracks and wear debris were examined by SEM micrographs and EDS spectrum and are shown in Fig. 7, 8 and 9. Since EDS analysis is a semiquantitative method and could not enable to detect light elements like carbon, nitrogen, oxygen and fluorine, the amount of the detected nitrogen and oxygen was more than the determined amounts.

The form of the generated wear tracks was

similar to each other. The EDS results revealed major tribochemical reaction in the coatings. The EDS analyses in some regions of the wear track in the coatings showed that the major element was Fe, which indicating a severe abrasion wear.

Comparison of the wear tracks in CrN coatings (Fig. 7) and (Ti, Cr)N coatings (Fig. 9) at a wear distance of 500m revealed that the groove formation and micro crack propagation in the (Ti, Cr)N coating is less than that in the CrN coating.

SEM observations showed that a severe abrasion and plastic deformation occurred in the coatings. The wear debris generated in TiN, CrN and (Ti, Cr)N samples showed a black brown, silver and reddish silver appearances, respectively. Size of wear debris generated in CrN coatings was larger than that generated from other two samples. The EDS analysis from debris showed that it contained a high level of oxygen that indicated severe tribo-chemical wear in the sample. Generally, a mixture of abrasive and oxidation reactions were the major wear mechanism in TiN, CrN and (Ti, Cr)N Coatings.

#### 4. CONCLUSION

Studies on the ternary (Ti, Cr)N and binary TiN and CrN films deposited by arc cathodic assisted PVD technique on tool steel (D6) showed the following conclusions:

The mechanical properties (hardness, Young's

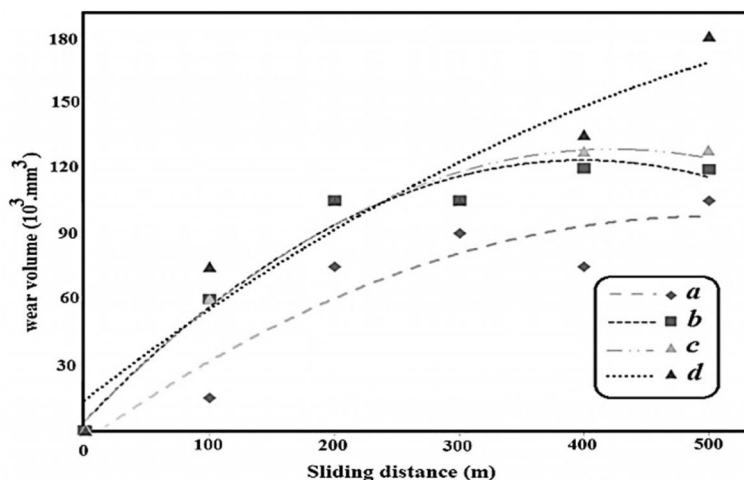


Fig. 6. The wear volume of specimens vs. sliding distance under the normal loads of 7N.



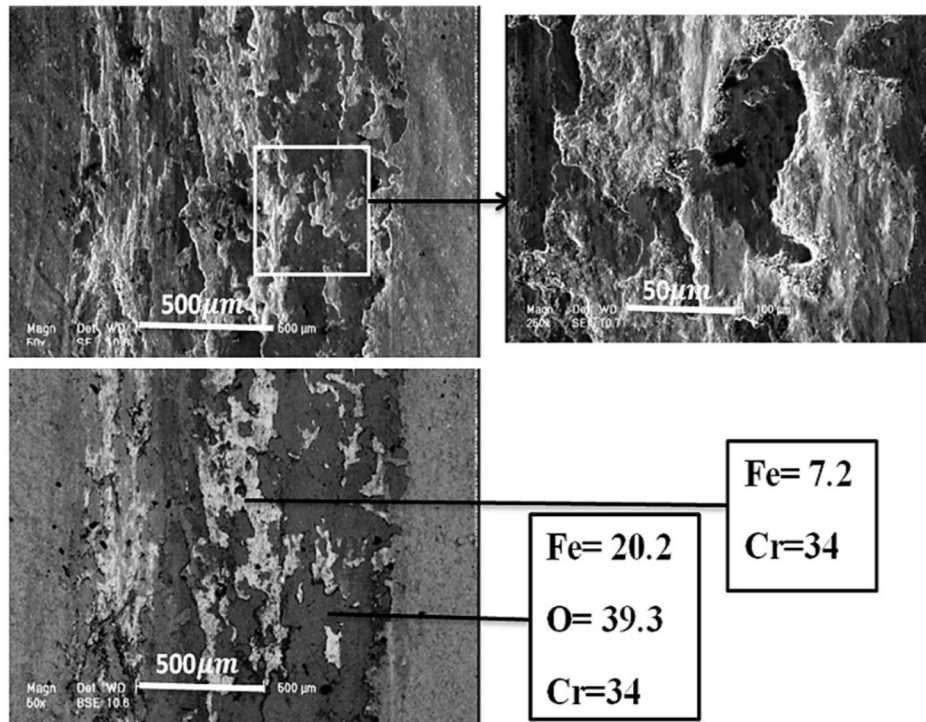


Fig. 7. Scanning electron micrographs (SE and BSE) of the wear track in CrN coatings at sliding distance of 500m

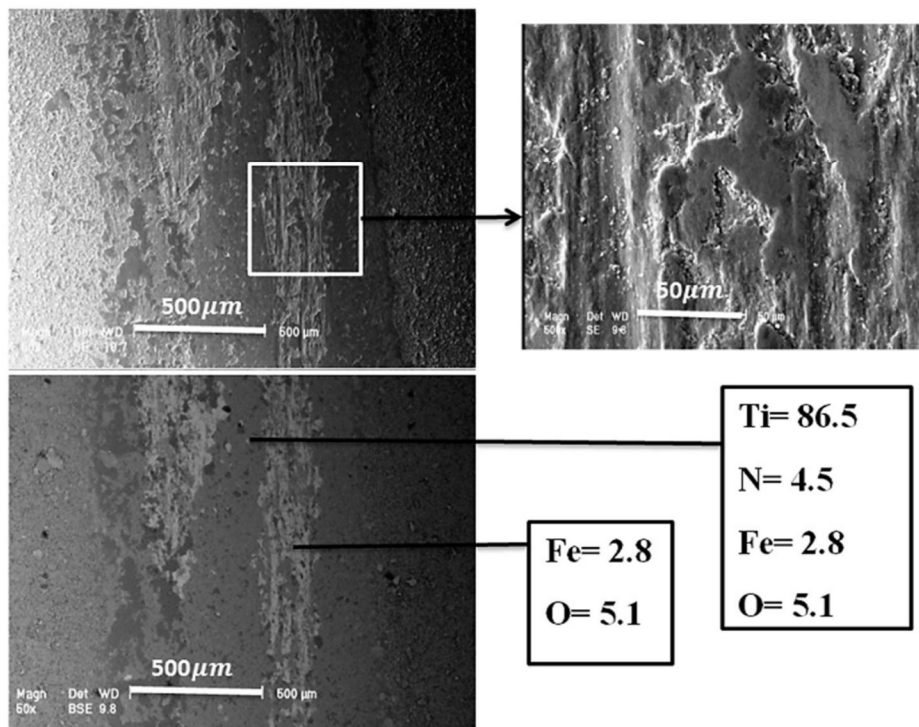


Fig. 8. Scanning electron micrographs (SE and BSE) of the wear track in TiN coatings at sliding distance of 500m.

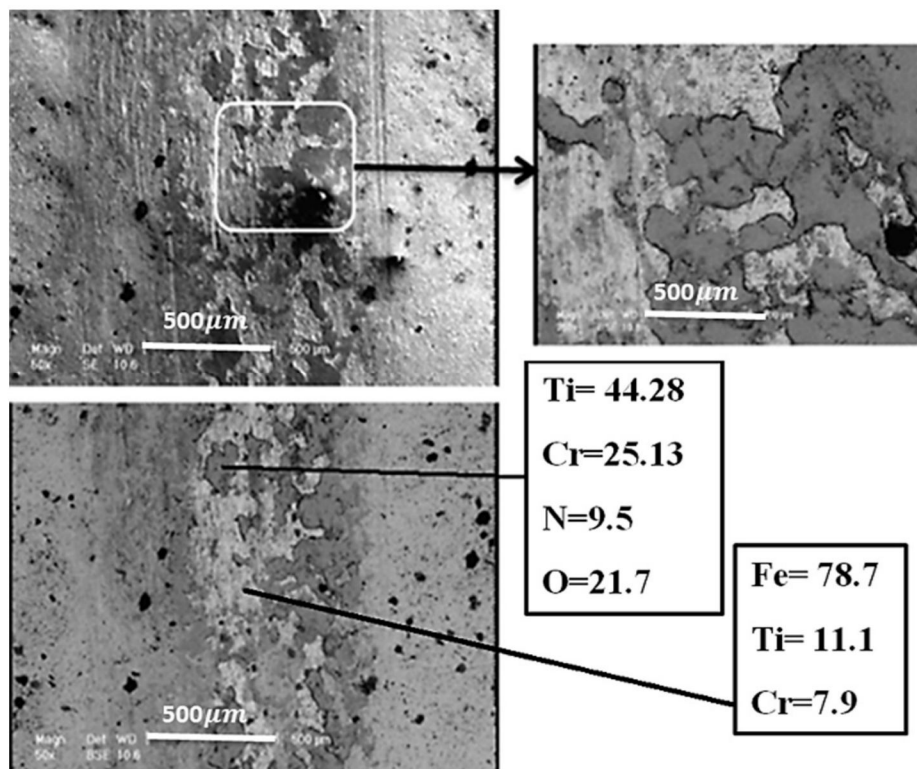


Fig.9. Scanning electron micrographs (SE and BSE) of the wear track in Ti, CrN coatings at sliding distance of 500m.

modulus, stiffness) of TiN coatings were higher than those of (Ti, Cr)N and CrN coatings.

Mechanical behavior of the (Ti, Cr)N coating was related to the Ti content of the coatings and hardness improved by decreasing the Ti content.

The coefficient of friction was reduced after coatings.

Amongst the three coatings materials, the TiN coating exhibited the highest wear resistance. On the other hand, the CrN coating showed the lowest wear resistance.

A mixture of the abrasive and oxidation wear was the dominant wear mechanism in the TiN, CrN and (Ti, Cr)N coatings.

## REFERENCES

1. Barshilia, H. C., Deepthi, B., Srinivas, G., Rajam, K. S., "Sputter deposited low-friction and tough Cr-Si<sub>3</sub>N<sub>4</sub> nanocomposite coatings on plasma nitrided M2 steel". *Vacuum*. 2012,

86, 1118-25.

2. Kovalev, A. I., Wainstein, D. L., Rashkovskiy, A. Y., Fox-Rabinovich, G. S., Yamamoto, K., Veldhuis, S., et al., "Impact of Al and Cr alloying in TiN-based PVD coatings on cutting performance during machining of hard to cut materials". *Vacuum*. 2009, 84, 184-7.
3. Panjan, P., Cekada, M., Panjan, M., Kek-Merl, D., "Growth defects in PVD hard coatings". *Vacuum*. 2009, 84, 209-14.
4. Warcholinski, B., Gilewicz, A., "Effect of substrate bias voltage on the properties of CrCN and CrN coatings deposited by cathodic arc evaporation". *Vacuum*. 2013, 90, 145-50.
5. Yongqiang, W., Xiaoxia, C., Xiubo, T., Chunzhi, G., Shiqin, Y., Zhiqiang, J., et al., "Effects of pulsed bias duty ratio on microstructure and surface properties of TiN films". *Vacuum*. 2013, 89, 185-9.
6. Huber, E., Hofmann, S., "High-temperature oxidation of (Ti, Pd)N and (Cr, Pd)N coatings



- studied with AES and XPS sputter depth profiling". *Vacuum*. 1994, 45, 1003-5.
7. Su, Y. L., Su, C. T., Yao, S. H., Yur, J. P., Hsu, C. A., Liu, T. H., "Friction and wear properties of Cr:(W<sub>x</sub>N<sub>0.1</sub>) coatings deposited by magnetron sputtering". *Vacuum*. 2006, 80, 1021-31.
  8. Budna, K. P., Neidhardt, J., Mayrhofer, P. H., Mitterer, C., "Synthesis–structure–property relations for Cr–B–N coatings sputter deposited reactively from a Cr–B target". *Vacuum*. 2008, 82, 771-6.
  9. Čekada, M., Panjan, P., Navinšek, B., Cvelbar, F., "Characterization of (Cr,Ta)N hard coatings reactively sputtered at low temperature". *Vacuum*. 1999, 52, 461-7.
  10. Ning-Kang, H., Yong, S., Ming-Hua, W., "Morphology, tungsten content and microhardness of electron beam melted Co<sub>0.6</sub>Cr<sub>0.4</sub>W coatings on steel". *Vacuum*. 1990, 40, 305-8.
  11. Schäfer, D., Hell, J., Eisenmenger-Sittner, C., Neubauer E., Hutter H., Kornfeind N., "Suppression of de-wetting of copper coatings on carbon substrates by metal (Cr, Mo, Ti) doped boron interlayers". *Vacuum*. 2009, 84, 202-4.
  12. Budzynski, P., Sielanko, J., Surowiec, Z., Tarkowski, P., "Properties of (Ti,Cr)N and (Al,Cr)N thin films prepared by ion beam assisted deposition". *Vacuum*. 2009, 83, Supplement 1, S186-S9.
  13. Mayrhofer, P. H., Willmann, H., Reiter A. E., "Structure and phase evolution of Cr–Al–N coatings during annealing". *Surface and Coatings Technology*. 2008, 202, 4935-8.
  14. Wang, L., Nie, X., Housden, J., Spain, E., Jiang, J. C., Meletis, E. I., et al., "Material transfer phenomena and failure mechanisms of a nanostructured Cr–Al–N coating in laboratory wear tests and an industrial punch tool application". *Surface and Coatings Technology*. 2008, 203, 816-21.
  15. Harris, S. G., Doyle, E. D., Vlasveld, A. C., Audy, J., Quick, D., "A Study of the Wear Mechanisms of Ti<sub>1-x</sub>Al<sub>x</sub>N and Ti<sub>1-x-y</sub>Al<sub>x</sub>Cr<sub>y</sub>N coated high-speed steel twist drills under dry machining conditions". *Wear*. 2003, 254, 723-34.
  16. Vishnyakov, V. M., Bachurin, V. I., Minnebaev, K. F., Valizadeh, R., Teer, D. G., Colligon, J. S., et al., "Ion assisted deposition of titanium chromium nitride". *Thin Solid Films*. 2006, 497, 189-95.
  17. Gåhlin, R., Bromark, M., Hedenqvist, P., Hogmark, S., Håkansson, G., "Properties of TiN and CrN coatings deposited at low temperature using reactive arc-evaporation". *Surf Coat Tech*. 1995, 76-77, Part 1, 174-80.
  18. Yan, W., Pun, C. L., Simon, G. P., "Conditions of applying Oliver–Pharr method to the nanoindentation of particles in composites". *Composites Science and Technology*. 2012, 72, 1147-52.
  19. Zhang, S., Lam Bui, X., Fu, Y., "Magnetron sputtered hard aC coatings of very high toughness". *Surf Coat Tech*. 2003, 167, 137-42.
  20. Huang, Z., Sun, Y., Bell, T., "Friction behaviour of TiN, CrN and (TiAl) N coatings". *Wear*. 1994, 173, 13-20.
  21. Ürgen, M., Eryilmaz, O. L., Cakir, A. F., Kayali, E. S., Nilufer, B., Işik, Y., "Characterization of molybdenum nitride coatings produced by arc-PVD technique". *Surf Coat Tech*. 1997, 94, 501-6.
  22. Urgan, M., Eryilmaz, O., Cakir, A., Kayali, E., Nilüfer, B., Işik, Y., "Characterization of molybdenum nitride coatings produced by arc-PVD technique". *Surf Coat Tech*. 1997, 94, 501-6.
  23. Chen, Y. H., Polonsky, I. A., Chung, Y. W., Keer, L. M., "Tribological properties and rolling-contact-fatigue lives of TiN/SiN<sub>x</sub> multilayer coatings". *Surface and Coatings Technology*. 2002, 154, 152-61.
  24. Huang, Z. P., Sun, Y., Bell, T., "Friction behaviour of TiN, CrN and (TiAl)N coatings". *Wear*. 1994, 173, 13-20.
  25. Aghajani, H., Soltanieh, M., Mahboubi, F., Rastegari, S., "Formation of a hybrid coating by the use of plasma nitriding and hard chromium electroplating on the surface of H11 hot work tool steel". *Iranian Journal of Materials Science and Engineering*. 2009, 6, 31-37.
  26. Bunshah, k. w. y., Sedakova, R. F., Dobrzański, E. L. A., "Micro Structural and Properties of TiAlN coating on high speed steel" .*Surface and Coatings Technolog* .1995, 73, 71-77.